Quasi-Harmonic Method for Calculating Vibrational Spectra from Classical Simulations on Multidimensional Anharmonic Potential Surfaces

Ronald M. Levy,* Olivia de la Luz Rojas,†

Department of Chemistry, Rutgers University, New Brunswick, New Jersey 08903

and Richard A. Friesner

Department of Chemistry, University of Texas, Austin, Texas 78712 *(Received: January 9, 1984)*

A quasi-harmonic approximation is described by which classical computer simulations on multidimensional potential surfaces can be used to estimate the effects of anharmonicity on vibrational spectra. A temperature-dependent effective quadratic Hamiltonian is parameterized by using the results of a classical computer simulation on the complete potential surface. The effective quasi-harmonic Hamiltonian defines a set of quasi-harmonic normal modes and frequencies which are rotated and shifted with respect to the harmonic values. As an illustration of the method, we report the results of a quasi-harmonic analysis of the potential surface of a small test molecule, butane. Temperature-dependent quasi-harmonic Hamiltonians are parameterized by using the results of Monte Carlo simulations at several temperatures. A novel aspect of the simulation is the use of normal-mode eigenvectors as the independent coordinates for Monte Carlo sampling. The results of the calculations are compared with reference calculations on the harmonic approximation to the butane potential surface and with experimental results concerning the temperature dependence of vibrational frequencies. The use of the quasi-harmonic normal modes as a reference system for the calculation of vibrational spectra from quantum Monte Carlo simulations is discussed.

I. Introduction

Computer simulations based on detailed atomic potential functions provide an extremely powerful method for studying the spectroscopic and statistical thermodynamic properties of large molecular systems. Since the results of these simulations are determined entirely by the properties of the potential and the potentials used for complex simulations necessarily require many approximations, there is a continuing effort to develop procedures to compare the results of simulations with a wide variety of experimental measurements on the corresponding real systems.[1-4] Such studies are not only useful for refining and ultimately verifying the accuracy of the potentials employed in the simulations but they also lead to deeper insights into the relationship between experimental probes and underlying molecular processes.[5] With regard to molecular dynamics simulations of biomolecules, the methodology required for comparing the simulation data with experimental results is rapidly advancing.[1-4]

Because of the very high sensitivity of high-resolution optical probes such as FTIR, resonance Raman, and coherent anti-Stokes Raman spectroscopy (CARS), these techniques contain a large amount of structural and dynamical information.[5-8] Within the harmonic approximation it is a straightforward matter to calculate optical properties from a model potential function. However, much of the interesting structural information that can be extracted from optical experiments involves understanding the origin of spectral shifts as a function of some experimentally adjustable parameter, often the temperature.[5-7] If computer simulations on realistic potential surfaces are to be useful for interpreting these optical experiments, it is essential that methods be developed which incorporate anharmonic effects on the calculated spectra since these effects often dominate the spectral changes. The standard approach to this problem has been to develop the potential in a perturbation series and to extract anharmonic coefficients from the positions of combination and overtone bands. This approach is practical only for relatively harmonic vibrations of the smallest molecules. As Warshel has pointed out,[9] the consistent force field (CFF) potentials we employ here have the advantage that anharmonicity is implicit in the consistent form of the potential, and explicit series expansions are therefore avoided. Semiclassical trajectories on these potential surfaces provide one possible approach to the anharmonic problem.[10,11] In this paper, we describe a method by which classical computer simulations can be used to estimate the effects of anharmonicity on vibrational spectra. The method involves a quasi-harmonic oscillator approximation.[12-14] The model Hamiltonian used to calculate the vibrational frequencies and normal modes is a quadratic function of the molecular coordinates and conjugate momenta. The results of classical Monte Carlo or molecular dynamics simulations on the complete anharmonic potential are used to parameterize the "quasi-harmonic" effective Hamiltonian. The Hamiltonian defines a set of quasi-harmonic normal modes (eigenvectors), frequencies (eigenvalues), and equilibrium positions. Spectral shifts due to anharmonicity can be immediately estimated from the quasi-harmonic normal modes and frequencies. Furthermore, the quasi-harmonic model is an extremely useful reference system for quantum-mechanical calculations of equilibrium and dynamic properties using quantum Monte Carlo methods.[15]

The formulation of a quasi-harmonic oscillator model using the results of molecular dynamics simulations was originally introduced in order to calculate thermodynamic and mechanical properties of macromolecules (polypeptides and proteins).[12-14] A systematic study of the quasi-harmonic oscillator method was not undertaken for these systems because of their very large size and the corresponding complexity of the calculations. In this paper we report the results of the quasi-harmonic analysis for the potential surface of a small test molecule, butane. The empirical potential for butane contains all the terms present in the potentials for the larger systems, viz bond stretching, bending, and torsional terms as well as nonbonded interactions. The butane model has

† Permanent address: Centro de Graduados, Instituto Technologico de Tijuana, Apdo Postal 1166, Tijuana B.C.

(1) R. M. Levy, M. Karplus, and P. G. Wolynes, *J. Am. Chem. Soc.*, **103**, 5998 (1981).
(2) R. M. Levy and A. Szabo, *J. Am. Chem. Soc.*, **104**, 2073 (1982).
(3) D. Fredkin, A. Komornicki, S. White, and K. Wilson, *J. Chem. Phys.*, **78**, 7077 (1983).
(4) R. M. Hochstrasser and H. P. Trommsdorff, *Acc. Chem. Res.*, **16**, 377 (1983).
(5) P. G. Debrunner and H. Frauenfelder, *Annu. Rev. Phys. Chem.*, **33**, 243 (1982).
(6) T. J. Kosic, R. Cline, Jr., and D. Dlott, *Chem. Phys. Lett.*, preprint.
(7) A. Warshel, *Annu. Rev. Biophys. Bioeng.*, **6**, 273 (1977).
(8) T. G. Shapiro, *Isr. J. Chem.*, **21**, 81 (1981).
(9) A. Warshel, *J. Chem. Phys.*, **55**, 3327 (1971).
(10) A. Warshel and M. Karplus, *Chem. Phys. Lett.*, **17**, 7 (1972).
(11) A. Myers, R. Mathies, D. Tannor, and E. J. Heller, *J. Chem. Phys.*, **77**, 3857 (1982).
(12) M. Karplus and J. Kushick, *Macromolecules*, **14**, 325 (1981).
(13) R. M. Levy, S. R. Srinivasan, W. Olson, and J. A. McCammon, *Biopolymers*, **23**, 1099 (1984).
(14) R. M. Levy, M. Karplus, J. Kushick, and D. Perahia, *Macromolecules*, in press.
(15) R. A. Friesner and R. M. Levy, *J. Chem. Phys.*, **80**, 4488 (1984).

0022-3654/84/2088-4233$01.50/0

TABLE I: Parameters[a] for the Butane Potential and Energy-Minimized[b] Coordinates for Trans and Gauche Butane

K_b = 250 kcal/(mol Å^2)	b_0 = 1.54 Å
K_θ = 120 kcal/(mol rad^2)	θ_0 = 112°
K_ϕ = 2.0 kcal/mol	
A = 1.21 × 10^6 kcal/(mol Å^{12})	
C = 6.60 × 10^2 kcal/(mol Å^6)	

coordinate	trans	gauche
b_1	1.540	1.543
b_2	1.540	1.545
b_3	1.540	1.543
θ_1	112.0	112.69
θ_2	112.0	112.69
ϕ	180.0	288.69

[a] Potential parameters obtained from ref 11. [b] 10 steepest descents plus 5 Newton–Raphson minimization steps starting from the reference trans and gauche geometries.

been used extensively for computer studies of both structural[16] and dynamic processes,[17,18] and in addition information is available concerning the temperature dependence of the vibrational spectrum for closely related systems.[19-21] In this paper we describe the method by which temperature-dependent quasi-harmonic potentials for butane are parameterized from the results of Monte Carlo simulations. A novel aspect of the simulation is the use of normal-mode eigenvectors as the independent coordinates for the Monte Carlo sampling. The numerical accuracy of the procedure is checked by performing Monte Carlo simulations on the harmonic part of the butane potential. To demonstrate the usefulness of the quasi-harmonic normal modes as a reference system for quantum Monte Carlo simulations, we compare the results of Monte Carlo simulations using both harmonic and quasi-harmonic normal modes as the choice of independent coordinates. The method is described in section II. The results and discussion are presented in section III.

II. Method

The form of the empirical potential used for the Monte Carlo simulations of butane is

$$V = \tfrac{1}{2}\sum_{\text{bonds}} K_{b_i}(b_i - b_{i0})^2 + \tfrac{1}{2}\sum_{\text{bond angles}} K_{\theta_i}(\theta_i - \theta_{i0})^2 + \tfrac{1}{2}K_\phi[1 + \cos(3\phi - \phi_{i0})] + \tfrac{1}{2}\left[\frac{A}{r^{12}} - \frac{C}{r^6}\right] \quad (1)$$

where the b_{i0}, θ_{i0}, and ϕ_{i0} are the equilibrium values for the isolated bond, bond angle, and torsional coordinates and the K_{b_i}, K_{θ_i}, and K_ϕ are the corresponding force constants. The last term of eq 1 corresponds to the van der Waals interaction between atoms that are not directly bonded. The parameters used in the present study are the same as those used in an earlier harmonic analysis for butane[12] and are listed in Table I. The methyl and methylene groups of the butane molecule were treated as extended atoms so that the model contained four interaction centers.[22] The conformation of the molecule is therefore determined by the 12 Cartesian coordinates or 6 internal coordinates (three bonds, two angles, and one torsional coordinate).

In the standard normal-model analysis,[23] the potential energy is expanded in a Taylor series about the equilibrium geometry and only the quadratic term is retained. The harmonic approximation to the Hamiltonian for the system can then be expressed as

$$\mathcal{H} = \tfrac{1}{2}\mathbf{p}_q\boldsymbol{G}\mathbf{p}_q + \tfrac{1}{2}\mathbf{q}\boldsymbol{F}\mathbf{q} \quad (2)$$

where $\boldsymbol{F}$ is the matrix of force constants, whose values are the second derivatives of the potential energy evaluated at the conformational minimum.[23] $\boldsymbol{G}$ is the kinetic energy matrix which is just a diagonal matrix of inverse masses when the problem is formulated in Cartesian coordinates. When the problem is formulated in internal coordinates, the form for $\boldsymbol{G}$ is more complicated. The explicit expressions for the kinetic and potential energy matrices are

$$G_{ij} = \sum_k \left[\frac{1}{m_k}\frac{dq_i}{dx_k}\frac{dq_j}{dx_k}\right]_{\{q_0\}} \qquad F_{ij} = \frac{d^2V}{\partial q_i\,\partial q_j}_{\{q_0\}} \quad (3)$$

where the generalized coordinates $\{q_0\}$ correspond either to internal or Cartesian coordinates. It should be noted that, in general, the normal-mode analysis involves approximations for both the kinetic and potential energies of the system. In the quasi-harmonic approximation the elements of $\boldsymbol{G}$ and $\boldsymbol{F}$ are parameterized from a computer simulation on the exact potential surface so that the ensemble average of specified properties matches as closely as possible the corresponding values calculated from the Monte Carlo or molecular dynamics trajectory. Here, as in previous applications of the quasi-harmonic method,[12-14] we shall retain the harmonic approximation for $\boldsymbol{G}$ of eq 3 and require that the quasi-harmonic matrix for $\boldsymbol{F}$ be constructed so that the classical second moments of the coordinate distributions equal the values obtained from the simulations on the exact potential. Other choices for the parameterization are possible. Using the second-moment criterion for the quasi-harmonic force constant matrix $\boldsymbol{F}^{\mathrm{QH}}$

$$\sigma_{ij} \equiv \langle (q_i - \langle q_i\rangle)(q_j - \langle q_j\rangle)\rangle = \frac{\int (q_i - q_{i0})(q_j - q_{j0})e^{-(1/2)\mathbf{q}\boldsymbol{F}^{\mathrm{QH}}\mathbf{q}}\,d\mathbf{q}}{\int e^{-(1/2)\mathbf{q}\boldsymbol{F}^{\mathrm{QH}}\mathbf{q}}\,d\mathbf{q}} \quad (4)$$

where σ is the matrix of second moments calculated from the Monte Carlo trajectory. The elements of σ can be expressed in terms of either internal coordinates or mass-weighted Cartesian coordinates. We have shown previously that the quasi-harmonic force constant matrix $\boldsymbol{F}^{\mathrm{QH}}$ is given by[14]

$$\boldsymbol{F}^{\mathrm{QH}} = k_{\mathrm{B}}T\sigma^{-1} \quad (5)$$

When σ is expressed in terms of internal coordinates, the matrix may be inverted by standard methods; when mass-weighted Cartesian coordinates are used, the matrix of second moments is singular so that it cannot be inverted directly. An inverse matrix can still be constructed from the $3N - 6$ nonzero eigenvalues and eigenvectors of σ in the mass-weighted Cartesian representation. When $\boldsymbol{U}$ is defined to be the $3N \times 3N - 6$ matrix whose $3N - 6$ columns are the eigenvectors of σ with nonzero eigenvalues, σ^{-1} in the mass-weighted Cartesian representation is given by

$$\sigma^{-1} = \boldsymbol{U}\lambda^{-1}\boldsymbol{U}^{\dagger} \quad (6)$$

where λ^{-1} is the diagonal matrix of inverse nonzero eigenvalues of σ. Both the harmonic and quasi-harmonic eigenvectors and frequencies are obtained as solutions to the secular equation

$$|\boldsymbol{GF} - \lambda\boldsymbol{I}| = 0 \quad (7)$$

The harmonic normal-mode solutions of the secular equation expressed both in a Cartesian and internal-coordinate basis were required for the calculations described below. The mass-weighted Cartesian eigenvectors for trans and gauche butane were obtained by solving the 12 × 12 secular equation. The internal coordinate components were then obtained from the mass-weighted Cartesian components:

$$\mathbf{Q}_k^i = \boldsymbol{T}\mathbf{Q}_k^x \quad (8)$$

where $\mathbf{Q}_k^x$ is the kth eigenvector in the mass-weighted Cartesian basis, $\mathbf{Q}_k^i$ is the kth eigenvector in the internal-coordinate basis,

(16) D. W. Reburtus, B. Berne, and D. Chandler, *J. Chem. Phys.*, **70**, 3395 (1979).
(17) R. M. Levy, M. Karplus, and J. A. McCammon, *Chem. Phys. Lett.*, **65**, 4 (1979).
(18) B. Bigot and W. Jorgensen, *J. Chem. Phys.*, **75**, 1977 (1981).
(19) B. Hudson, A. Warshel, and R. Gordon, *J. Chem. Phys.*, **61**, 2929 (1974).
(20) K. A. Strong, Report IW-1237, AEC, Washington, DC, 1974.
(21) M. Kobayashi and H. Tadokoro, *J. Chem. Phys.*, **66**, 1258 (1977).
(22) R. M. Levy and M. Karplus, *Biopolymers*, **18**, 2465 (1979).
(23) E. B. Wilson, J. C. Decius, and P. C. Cross, "Molecular Vibrations", McGraw-Hill, New York, 1955.

TABLE II: Harmonic Normal-Mode Frequencies and Eigenvectors For Trans and Gauche Butane

			Trans Butane			
frequency, cm^{-1}	119	406	437	901	1002	1044
eigenvector component[a]	Q_1	Q_2	Q_3	Q_4	Q_5	Q_6
Δb_1	-3×10^{-9}	-2×10^{-7}	-7×10^{-2}	0.3	1.9×10^{-2}	0.25
Δb_2	-6×10^{-9}	6×10^{-17}	-8×10^{-2}	-2×10^{-17}	−0.35	−0.10
Δb_3	-3×10^{-7}	-2×10^{-7}	-7×10^{-2}	−0.3	1.9×10^{-2}	0.25
$\Delta\theta_1$	-9×10^{-7}	−9.7	−7.2	-6.3×10^{-7}	12.0	−12.7
$\Delta\theta_2$	-9×10^{-7}	9.7	−7.2	6.3×10^{-7}	12.0	−12.7
$\Delta\phi$	21	-9×10^{-15}	-2×10^{-5}	9.1×10^{-18}	7.0×10^{-5}	1.7×10^{-5}
			Gauche Butane			
frequency, cm^{-1}	147	419	599	863	964	1035
eigenvector component	Q_1	Q_2	Q_3	Q_4	Q_5	Q_6
Δb_1	2.1×10^{-3}	3.4×10^{-2}	-8.0×10^{-2}	0.18	0.25	−0.18
Δb_2	1.3×10^{-3}	7.0×10^{-2}	2.1×10^{-17}	0.17	-8.7×10^{-18}	0.33
Δb_3	2.1×10^{-3}	3.4×10^{-2}	8.0×10^{-2}	0.18	−0.25	−0.18
$\Delta\theta_1$	8.2×10^{-2}	8.35	−12.8	−10.1	−10.5	−3.95
$\Delta\theta_2$	8.2×10^{-2}	8.35	12.8	−10.1	10.5	−3.95
$\Delta\phi$	22.6	14.3	1.8×10^{-15}	7.45	7.8×10^{-16}	0.74

[a] Bond length displacements in angstroms; bond angle and torsional displacements in degrees.

and $\boldsymbol{T}$ is the matrix of partial derivatives $(1/m^{1/2})\partial q_i/\partial x_j$.

The Monte Carlo procedure for constructing the quasi-harmonic force constant matrix involves sampling the potential surface in the region of the energy-minimum conformation. It is very useful to choose the set of normal coordinates $\{\mathbf{Q}_k^x\}$ or $\{\mathbf{Q}_k^i\}$ as the independent coordinates for the Monte Carlo trajectory. Sampling in these coordinates simplifies the construction of the second-moment matrix because the displacement vectors do not contain translational or rotational components. More importantly, these are the natural coordinates to choose for quantum Monte Carlo simulations (see below and ref 15). Monte Carlo simulations at a series of temperatures between 5 and 300 K were performed on both the harmonic and exact butane potential surfaces. The Metropolis acceptance probability for a step on the harmonic (W^H) and exact (W^E) potentials are respectively

$$W^H(\mathbf{Q}_k \rightarrow \mathbf{Q}_k') = e^{-(\omega_k^2/2k_BT)(|\mathbf{Q}_k'|^2-|\mathbf{Q}_k|^2)} \quad \text{if } |\mathbf{Q}_k'|^2 - |\mathbf{Q}_k|^2 > 1$$
$$= 1 \text{ otherwise} \tag{9a}$$

$$W^E(\mathbf{Q}_k \rightarrow \mathbf{Q}_k') = e^{-(1/k_BT)(V\{\mathbf{Q}'\}-V\{\mathbf{Q}\})} \quad \text{if } V\{\mathbf{Q}'\} > V\{\mathbf{Q}\}$$
$$= 1 \text{ otherwise} \tag{9b}$$

$V\{\mathbf{Q}'\}$ is a function of all the normal coordinates since for the exact potential, $\mathbf{Q}_k$ is coupled in principle to all the other normal coordinates. Monte Carlo step lengths were adjusted to achieve ~40–60% acceptance; for each trial displacement along mode i, the displacement was scaled by the inverse frequency (ω_{max}/ω_i), so that smaller steps were taken along the high-frequency modes than the low ones. For Monte Carlo sampling along the harmonic surface, calculations were compared with $\mathbf{Q}_k$ expressed both in internal and mass-weighted Cartesian coordinates. Because the exact potential V contains a van der Waals term which depends on the interatomic distance R between non-bonded atoms, it is not convenient to express the total energy in terms of internal coordinates, so that, for the calculations on the exact potential, only mass-weighted Cartesian eigenvectors were used. One pass of the Monte Carlo trajectory consisted of trial displacements along each of the six normal coordinates. A 50 000-pass Monte Carlo trajectory on the harmonic surface with the set of six $\{\mathbf{Q}_k^i\}$ chosen as the independent coordinates required ~6 CPU min on a VAX 11/780. For the calculations on the exact potential using the set of six $\{\mathbf{Q}_k^x\}$ as the independent coordinates, 50 000 passes required ~20 CPU min on a VAX 11/780. The results of the model calculations are presented in the following section.

III. Results and Discussion

The energy-minimized coordinates for trans and gauche butane were obtained by performing 10 steepest descent followed by 10 Newton–Raphson minimization steps on the butane potential surface starting from initial coordinates selected near the expected equilibrium geometry. The final root-mean-square derivatives were less than 10^{-5} for both minimizations. The energy-minimized coordinates are listed in Table I. For the trans conformation the bond lengths and angles at the energy minimum are equal to the geometric reference "zero" values b_0 and θ_0 of the potential function (eq 1) whereas at the gauche minimum the bond lengths and angles have increased slightly over the reference values. This opening up of the bond lengths and angles is due to the van der Waals repulsion between the terminal methyl groups, which is negligible in the trans conformation. The harmonic normal-mode frequencies and eigenvectors for trans and gauche butane obtained by solving the secular equation using $\boldsymbol{F}^H$ (eq 3) are shown in Table II. For trans butane the frequencies range between 119 and 1044 cm^{-1}. It is apparent from the eigenvectors that the lowest frequency vibrational mode for trans butane is a pure torsional deformation, the second lowest mode (406 cm^{-1}) is a pure bond angle deformation, while all three types of coordinates are mixed in the remaining four modes (437, 901, 1002, and 1044 cm^{-1}). The gauche butane vibrational frequencies and modes are significantly different from the trans modes. There are no "pure" gauche modes, although the lowest frequency gauche vibration is predominantly a torsional deformation. In contrast to trans butane for the second and fourth lowest frequency gauche modes (419 and 863 cm^{-1}), the torsional and bond angle motions are strongly mixed. The harmonic normal-mode results presented in Table II provide a reference for comparison with the quasi-harmonic normal modes calculated from the Monte Carlo trajectories.

In order to test the accuracy of the procedure for constructing a quasi-harmonic potential from computer simulations, a series of Monte Carlo trajectories for trans butane were carried out by using the harmonic approximations to the complete potential. That is, the potential surface was assumed to have the form

$$V\{\mathbf{Q}_k\} = \sum_k \tfrac{1}{2}\omega_k^2|\mathbf{Q}_k|^2 \tag{10}$$

where the eigenvalues and eigenvectors are the trans butane values listed in Table II, and eq 9a was used for the Metropolis acceptance test. Monte Carlo trajectories on the harmonic surface were run at four temperatures: 5, 100, 200, and 300 K. The quasi-harmonic frequencies corresponding to the quasi-harmonic normal modes constructed from these Monte Carlo trajectories are listed in Table III. At each temperature separate trajectories were run with both $\mathbf{Q}_k^x$ and $\mathbf{Q}_k^i$ as the independent coordinates. For all the trajectories, the quasi-harmonic force constant matrix was constructed from the matrix of *internal-coordinate* second moments calculated from the simulation. Since the simulations were run on the harmonic potential surface, the inverse of the second-moment matrix should be proportional to the matrix of

TABLE III: Quasi-Harmonic Frequencies[a] Calculated for Trans Butane from Monte Carlo Trajectories on the *Harmonic* Potential Surface

5 K	100 K	200 K	300 K
119[b]	122[b] (2)[d]	116[b] (2.5)	119[b]
407	401	404	406
436	439	441	435
905	872 (3)	909	900
1000	993	982 (2)	1008
1057	1034	1060 (1.5)	1057
118[c]	123[c]	121[c]	122[c]
407	411	408	406
437	428	432	424
908	898	902	911
1000	982 (2)	952 (5)	919 (8)
1053	1020 (2.3)	1023 (2)	1007 (4)

[a] Frequencies in cm^{-1}. [b] Monte Carlo trajectories with $\{Q_k(\text{internal})\}$ as independent coordinates. [c] Monte Carlo trajectories with $\{A_k(\text{mass-weighted Cartesian})\}$ as independent coordinates. [d] Numbers in parentheses indicate percent deviation from harmonic normal-mode eigenvalues; only deviations greater than 1% indicated.

second derivatives of the potential evaluated at the energy minimum; the quasi-harmonic normal modes constructed from the Monte Carlo trajectories should reproduce the harmonic normal-mode frequencies and eigenvectors (Table I) calculated from the second-derivative matrix. Differences between the quasi-harmonic and harmonic normal modes must be attributed to inadequate Monte Carlo sampling statistics or numerical problems associated with the construction of the quasi-harmonic force constant matrix from the trajectory. Statistics from three separate 50 000-step Monte Carlo trajectories at each temperature were averaged to construct the quasi-harmonic normal modes whose frequencies are listed in Table III.

The agreement between the harmonic and quasi-harmonic frequencies calculated from the Monte Carlo trajectories with $\{Q_k^I\}$ chosen as the set of independent coordinates is very good (see Table III). The largest deviation between a harmonic and quasi-harmonic mode is 3% (mode 4 at 100 K) and most of the modes agree with the harmonic reference values to within 1%. Quasi-harmonic frequencies calculated from trajectories using $\{Q_k^x\}$ as the set of independent coordinates are also reported in Table III. Since for this study the quasi-harmonic force constants were always calculated from the matrix of second moments of *internal-coordinate* fluctuations, when the normal coordinates used for the Monte Carlo sampling are expressed in a Cartesian basis, the harmonic and quasi-harmonic results need not agree, even when the potential is assumed to be harmonic (eq 10). The approximation that is being tested in this series of calculations is the approximation of the kinetic energy matrix at each point on the potential surface by its value at the minimum, which depends upon the accuracy of eq 8. It is apparent from the results of Table III that this is a reasonably good approximation for the geometries accessible to trans butane between 5 and 300 K. However, approximations involved in the kinetic energy expression (eq 3) do appear to lead to a small but systematic error in the calculated frequency for one of the modes (mode 5) for which the harmonic and quasi-harmonic values differ by 8% at 300 K.

The quasi-harmonic frequencies calculated for trans and gauche butane from Monte Carlo simulations on the exact butane potential at 100, 200, and 300 K are listed in Table IV. In order to prevent the Monte Carlo trajectories from sampling multiple minima, infinite barriers were placed at dihedral angle values corresponding to maxima in the torsional potential. For both trans and gauche butane, five of the six quasi-harmonic frequencies agree with the harmonic values to within 1%. Only for the lowest frequency modes of the two conformations does the anharmonic nature of the potential significantly shift the frequency. For trans butane, the lowest frequency mode is a pure torsion, and for gauche butane, it is also largely a torsional displacement with a very small angle bending component. For trans butane at 300 K the quasi-harmonic frequency is decreased by 25% compared with the harmonic value (91 cm^{-1} (quasi-harmonic) vs. 119 cm^{-1} (harmonic)) while for gauche butane the torsional mode is decreased by 33% to 99 cm^{-1} (the harmonic frequency is 147 cm^{-1}). The torsional potential for butane is clearly very anharmonic (eq 1), and the decreasing curvature of the torsional potential away from the minimum would tend to decrease the effective frequencies obtained by fitting the exact potential along this coordinate to a quadratic form (Figure 1). For the model butane potential studied (eq 1) the bond length and angle terms are harmonic. The higher frequency modes are therefore expected to be largely harmonic. However, all three types of internal coordinates are, in principle, coupled *anharmonically* through both the kinetic energy matrix and the van der Waals potential. From the normal-coordinate results it is apparent that for trans butane the torsional coordinate is uncoupled from the other coordinates (the torsional coordinate is a good normal coordinate) while for gauche butane there is some harmonic coupling between the dihedral angle and the bond angles. It is clear from the quasi-harmonic analysis that the anharmonic coupling among the normal modes for both trans and gauche butane is extremely weak on those portions of the potential surface accessible to the molecule at 300 K.

TABLE IV: Quasi-Harmonic Frequencies[a] Calculated from Monte Carlo Trajectories on the *Exact* Potential Surface for Trans and Gauche Butane

trans			gauche
100 K	200 K	300 K	300 K
113 (5)	102 (17)	91 (25)	99 (33)
407	406	407	419
435	437	436	602
899	911	892	857
1008	1014	1002	966
1045	1055	1043	1034

[a] Frequency in cm^{-1}. [b] Monte Carlo trajectories constructed with $\{Q_k(\text{mass-weighted Cartesian})\}$ as independent coordinates. [c] Numbers in parentheses indicate percent deviation from harmonic normal-mode eigenvalues; only deviations greater than 1% indicated.

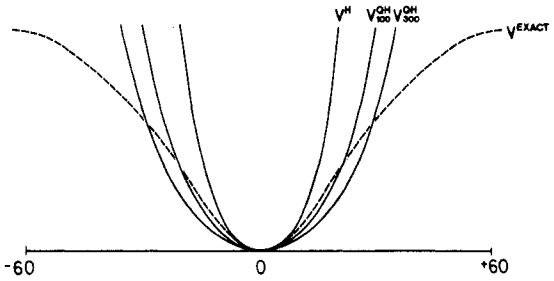

Figure 1. Schematic illustration of the exact potential V^{exact}, the harmonic approximation V^H, and quasi-harmonic approximations at 100 K, V^{QH}_{100}, and 300 K, V^{QH}_{300}, for the torsional coordinate Q of trans butane. The anharmonicity of the exact potential results in the decreasing curvature of the quasi-harmonic potentials with increasing temperature.

In the quasi-harmonic model, the anharmonicity of the exact potential surface can affect the quasi-harmonic normal modes in two ways: (1) the quasi-harmonic frequencies are shifted with respect to the harmonic values, and (2) the quasi-harmonic eigenvectors are rotated with respect to the harmonic eigenvectors. It is apparent from the results presented above that only the lowest frequency modes of trans and gauche butane are significantly affected by anharmonicity, and therefore the quasi-harmonic coordinates for this model system cannot be significantly rotated with respect to the harmonic coordinate system. In general, however, the rotation of the normal-mode coordinates can significantly affect experimental intensities. The rotation of the quasi-harmonic potential surface with respect to the harmonic surface can be expressed in terms of a (Duschinsky) rotation matrix. This is completely analogous to the description of the rotation of vibrational coordinates between two different electronic surfaces. We have calculated the rotation matrix elements required to expand the quasi-harmonic eigenvectors in the harmonic basis set in order to verify the accuracy of our method for cal-

TABLE V: "Duschinsky" Matrices for Rotation between Harmonic and Quasi-Harmonic Potential Surfaces Constructed from Monte Carlo Trajectories

	harmonic					
quasi-harmonic	Q_1	Q_2	Q_3	Q_4	Q_5	Q_6
	(a) Harmonic Trans Butane Potential Surface					
Q_1	0.999	−0.007	0.002	0.002	0.000	−0.002
Q_2	0.007	0.999	0.040	−0.007	0.004	−0.001
Q_3	0.002	0.040	−0.999	−0.010	0.000	0.000
Q_4	−0.002	0.008	−0.010	0.999	−0.067	−0.039
Q_5	−0.000	−0.004	−0.001	0.070	0.999	−0.024
Q_6	−0.018	0.001	0.000	−0.040	−0.021	0.999
	(b) *Exact* Trans Butane Potential Surface					
Q_1	0.999	0.000	−0.002	0.000	0.000	0.001
Q_2	0.000	0.999	0.076	0.003	0.003	−0.002
Q_3	−0.001	−0.076	−0.999	0.004	−0.006	0.005
Q_4	0.000	0.003	0.003	0.999	−0.034	−0.025
Q_5	0.000	0.002	−0.007	0.031	0.993	−0.117
Q_6	0.000	0.001	−0.004	−0.029	0.116	−0.993

culating quasi-harmonic normal modes. In order to calculate the overlap between the harmonic and quasi-harmonic eigenvectors, it is necessary to normalize the quasi-harmonic eigenvectors which are obtained as solutions to the secular equation by using the quasi-harmonic force constant matrix. After normalization, the rotation matrix elements a_{ij} are just equal to the dot product of the harmonic eigenvectors with the quasi-harmonic eigenvectors, both expressed in the internal coordinate basis:

$$a_{ij} = \mathbf{Q}_i^{\mathrm{H}}\mathbf{Q}_j^{\mathrm{QH}} \tag{11}$$

The "Duschinsky" matrices for rotation between the harmonic and quasi-harmonic potential surfaces constructed from two of the Monte Carlo trajectories for trans butane are shown in Table V. As expected, the matrices are nearly diagonal; the largest off-diagonal elements are between modes that are close in frequency. For the test calculation using the harmonic surface for the Monte Carlo simulation, the largest off-diagonal component is 0.07 for the overlap between the harmonic and quasi-harmonic modes 4 and 5, while for the Monte Carlo trajectory on the exact trans surface at 300 K, the largest overlap is 0.12 between modes 5 and 6. This result suggests that the calculation of the quasi-harmonic eigenvectors is inherently less accurate than the eigenvalues and that for the present calculations the error in the eigenvectors can be as large as ~10%. Since both the energy and the infrared absorption intensity depend on the square of the eigenvectors, the present level of precision in the eigenvectors may be adequate for future applications of the method. It is possible to make some comparison between the quasi-harmonic calculations reported here and the experimentally determined temperature dependence of the vibrational frequencies for butane and related systems. The most complete study of the temperature dependence of the butane frequencies comes from neutron scattering experiments.[19,20] In agreement with the present calculations only the lowest frequency mode is found to depend on temperature. The intensity maximum for this torsional mode is observed to shift to lower frequencies with increasing temperature, decreasing from 150 cm^{-1} at 106 K to 130 cm^{-1} at 172 K.[20] Both the direction of the observed shift and the magnitude are in agreement with the quasi-harmonic model results. Unfortunately, it is not possible to unambiguously separate intramolecular from intermolecular effects. At the lower temperature (106 K) butane is a polycrystalline solid with an all-trans conformation, while at the higher temperature butane is a liquid and presumably consists of a trans/gauche mixture. Since the harmonic torsional frequency for gauche butane is greater than trans, the experimentally observed temperature dependence cannot be due to the mixture of conformers. More subtle intermolecular effects could contribute to the observed shifts; it might be possible to estimate the magnitude of these effects by performing a harmonic analysis on the butane torsional potential of mean force.[17] With regard to related systems, detailed temperature-dependent infrared and Raman data have been collected for a series of *n*-paraffins, including orthorhombic polyethylene.[21] Several of the lattice modes show a strong temperature dependence for this polymer; one of the librational modes decreases from 140 cm^{-1} at 90 K to 100 cm^{-1} at 300 K. The authors note that, for a quantitative interpretation of the temperature dependence of the lattice mode frequencies, evaluation of the contribution of anharmonicity to each mode as well as the change in lattice cell constants must be taken into account.

The theoretical analysis of optical spectra depends ultimately on the calculation of quantum-mechanical time correlation functions. Within the harmonic or quasi-harmonic framework both the classical and quantum time correlation functions are very simple to calculate. Analysis of anharmonic effects on vibrational spectra beyond the quasi-harmonic model remains a difficult problem since a more detailed analysis requires explicit consideration of the quantum dynamics of anharmonic systems. We have demonstrated[15] that the quasi-harmonic model is an excellent reference system for the evaluation of quantum equilibrium correlation functions using discretized path integral methods, and work on the time-dependent problem is under way. We have shown that the quasi-harmonic discretized path integral (QHDPI) calculation converges most rapidly for a quadratic reference system which minimizes the energy difference $V'(\{\mathbf{Q}\})$ between the exact and quasi-harmonic energy:

$$V'(\{\mathbf{Q}\}) = V^{\mathrm{E}}(\{\mathbf{Q}\}) - V^{\mathrm{QH}}(\{\mathbf{Q}\}) \tag{12}$$

For illustrative purposes we have carried out a classical Monte Carlo simulation at 300 K on the exact butane trans potential using as independent coordinates the set $\{Q_k^{\mathrm{QH}}\}$ which were constructed from a previous Monte Carlo simulation. The quasi-harmonic eigenvectors in the Cartesian basis are given by

$$\mathbf{Q}_k^{x,\mathrm{QH}} = \sum_i a_{ik}\mathbf{Q}_i^{x,\mathrm{H}}$$

where the a_{ik} are the Duschinsky matrix elements.

We have evaluated the average energy difference between the exact and reference systems over the simulation $V' = \langle H - H^\circ \rangle$ using both the harmonic Hamiltonian and the quasi-harmonic Hamiltonian as the choice of reference system, H°. The use of the quasi-harmonic reference for the butane potential was found to decrease the average residual classical energy difference V' by 33% compared with the case of the standard harmonic reference. It is expected therefore that the use of the quasi-harmonic reference for butane will lead to faster convergence of QHDPI calculations than will the harmonic reference. Comparison of the classical results for butane described in this paper with QHDPI calculations for butane will be described in a future paper.

IV. Conclusion

The quasi-harmonic method of parameterizing a quadratic temperature-dependent Hamiltonian from the results of a classical simulation on an anharmonic potential surface provides a way of partially incorporating anharmonic effects in the calculation of vibrational spectra. Analysis of the temperature dependence of the spectral shift and rotation matrices for the quasi-harmonic

normal modes will be extremely useful for interpreting the temperature dependence of both vibrational infrared and resonance Raman spectra for a large variety of systems of interest. Applications of the method described here and its quantum-mechanical extension to a series of biological chromophores are currently under way.

Acknowledgment. We thank Dr. A. Szabo for suggesting how to calculate the quasi-harmonic force constant matrix in the Cartesian representation. This work has been supported by NIH Grant GM30580 (R.M.L.), the donors of Petroleum Research Fund, administered by the American Chemical Society (R.M.L.), the Busch Foundation (R.M.L.), and the Robert A. Welch Foundation (R.A.F.). R. M. Levy and R. A. Friesner are Alfred P. Sloan Fellows. R. M. Levy is the recipient of an NIH Research Career Development Award.

Registry No. Butane, 106-97-8.

Activation of Chemical Reaction by Impact of Molecules on a Surface. 2. The Decomposition of Tetramethyldioxetane

F. J. Bottari and E. F. Greene*

Chemistry Department,[1] Brown University, Providence, Rhode Island 02912 *(Received: January 13, 1984)*

Molecules of tetramethyldioxetane (TMD) in a beam from a supersonic nozzle are accelerated up to kinetic energies E_k of 170 kJ mol^{-1} by being seeded into an excess of H_2 carrier gas. Light emitted when the molecules are suddenly brought to rest by collision with various surfaces is detected by a photomultiplier tube. The amount of light emitted varies with the nature and temperature of the surface as well as the temperature of the nozzle. It is greatest for surfaces of poly(tetrafluoroethylene) and a fluorinated copolymer of ethylene and propylene, but the yields are low, being no greater than 2×10^{-7} photons per molecule of TMD when the nozzle and surface are at room temperature. Other surfaces studied are stainless steel, glass, polyethylene, a polyimide, poly(vinylidene chloride), polyethylene terephthalate, and paraffin. Activation by impact permits the transfer of a large amount of kinetic to internal energy of a molecule in a single collision, so experiments of this kind should be helpful in the study of the detailed nature of chemical reactions.

Introduction

An earlier report from this laboratory[2] described experiments in which potentially reactive molecules were accelerated to high speeds and then rapidly brought to rest by collision with a stationary surface. The object was to study the conversion of the kinetic energy E_k into the molecules' internal energy E_{int} brought about by their collisions with the surface. The acceleration was produced by seeding the molecules at low concentrations into a carrier gas, usually H_2, and permitting the mixture to expand through a nozzle held at a temperature T_N. The clearest results were for the decomposition of $W(CO)_6$. When E_k exceeded a threshold value approximately equal to the binding energy of three CO molecules, the beam left a measurable amount of a nonvolatile deposit on the surface it hit. The latter was a glass slide held at a temperature T_s. Thus, the experimental variables were T_N, E_k, and T_s. T_N represented an upper limit for the internal temperature of the molecules in the beam because they cooled by an undetermined amount during the expansion.

Relatively little work of this kind has been done as yet. A similar experiment was carried out by Fenn[3] and his associates, who accelerated cyclopropane molecules seeded into a He carrier gas. They deduced an effect of E_k indirectly in that it caused a change in the activation energy E_a they found for the isomerization to propylene. (E_a was found from the variation of T_s.) That a single collision of fast molecules with a surface can produce high levels of vibrational excitation in a diatomic molecule has been shown by Kolodney and Amirav,[4] who observed the dissociation of I_2 after its collision with a sapphire surface. They found that the yield of I atoms was proportional to $(E_k - E_D)^2$ above a threshold energy equal to the bond energy $E_D = 1.54$ eV. Elber and Gerber,[5] in related theoretical work, have used classical trajectories to show that the angular and velocity distributions of scattered atoms A, produced when a diatomic molecule A_2 strikes a surface, are notably different from those expected when A itself is the incoming particle. This work shows that increases in E_{int} of molecules that collide with surfaces can be studied in detail. If suitable techniques can be developed for its use, this may become a useful way to learn how molecules are stimulated to undergo reactions. The present paper describes the decomposition of tetramethyldioxetane (TMD) activated by collision with a variety of surfaces. We presume the reaction occurring is the well-known one[6-10]

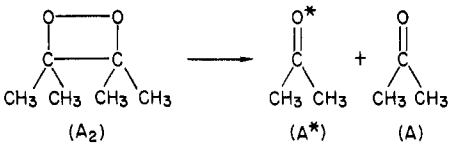

(1)

followed by

$$A^* \rightarrow A + h\nu$$

(1) Supported in part by the Department of Energy, Office of Basic Energy Sciences.

(2) Connolly, M. S.; Greene, E. F.; Gupta, C.; Marzuk, P.; Morton, T. H.; Parks, C.; Staker, G. *J. Phys. Chem.* **1981**, *85*, 235. Corrections should be made as follows: in Figure 2 the carrier gas pressures should all be increased by a factor of 10; in Figure 3 the abscissa should have units 10^4 Pa; in Figure 4 the caption should have the third nozzle diameter be 0.095 mm, and the second curve from the top should have filled-in circles indicating a CCl_4 vapor pressure of 180 Pa while the open symbols are for a pressure of 1100 Pa.

(3) Prada-Silva, G.; Kester, K.; Löffler, D.; Haller, G. L.; Fenn, J. B. *Rev. Sci. Instrum.* **1977**, *48*, 897. Prada-Silva, G.; Löffler, D.; Halpern, B. L.; Haller, G. L.; Fenn, J. B. *Surf. Sci.* **1979**, *83*, 453.

(4) Kolodney, E.; Amirav, A. *J. Chem. Phys.* **1983**, *79*, 4648.

(5) Elber, R.; Gerber, R. B. *Chem. Phys. Lett.* **1983**, *97*, 4.

(6) Turro, N. J.; Lechtken, P.; Schore, N. E.; Schuster, G.; Steinmetzer, H. C.; Yekta, A. *Acc. Chem. Res.* **1974**, *4*, 97.

(7) Wilson, T. *Int. Rev. Sci.: Phys. Chem., Ser. Two* **1976**, *9*, 265.

(8) Adam, W. *Adv. Heterocycl. Chem.* **1977**, *21*, 437.

(9) Adam, W.; Curci, R. *Chim. Ind. (Milan)* **1981**, *63*, 20.

(10) (a) Bogan, D. J. In "Chemical and Biological Generation of Excited States"; Adam, W., Cilento, G. Eds.; Academic Press: New York, 1982; Chapter 2. (b) Kopecky, K. R. In ref 10a; Chapter 3. (c) Adam, W. In ref 10a; Chapter 4. (d) Adam, W.; Zinner, K. In ref 10a; Chapter 5.

0022-3654/84/2088-4238$01.50/0